Paper published in International Journal of Heat and Technology, Vol. 23, N°1, pp 61-68 (2005)

HEAT EXCHANGE MODELING OF A GRATE CLINKER COOLER AND ENTROPY PRODUCTION ANALYSIS

D. Touil [1], H. F Belabed [2], C. Frances[*1], S. Belaadi [3]

[1] Laboratoire de Génie Chimique, UMR CNRS 5503 ENSIACET/ INP, BP 1301, 31106 Toulouse Cedex 01, France
[2] Department of Industrial Chemistry, Saâd Dahleb University, Route de Soumâa, BP 270, 09000 Blida, Algeria
[3] Department of Industrial Chemistry, USTHB, Bab-Ezzouar, BP 32, 16000 Algiers, Algeria.

[*]Corresponding author: Christine.Frances@ensiacet.fr

ABSTRACT

The concept of the exergy analysis is applied to a grate cooler of a cement production facility. The cooling of the clinker is modelled by a gas-solid series of cross-current contacting stages fully mixed for the calculation of the temperatures of the clinker and the air with their thermodynamic properties along the cooler. The equation of the production of entropy developed in the case of this representation reveals various adimensional parameters. The study of the sensitivity of the entropy generation number by tests of simulation in real operating conditions of the cooler shows the importance of the inlet temperature ratio and the number of stages cross-current contacting.

1. INTRODUCTION

The Mitidja Cement Compagny (SCMI) initiated a research program in order to improve quality of the energy consumption in the process of clinker burning which is a determining step in the manufacture of cement. The analysis of this process by the two first principles of thermodynamics highlighted the importance of the energy degradation in this system [1-4]. Several research tasks are currently directed towards the comprehension and the control of the mechanisms responsible for the degradation of energy to minimize the system losses [5]. The system of clinker burning is composed of three parts: the grate cooler, the rotary kiln and the suspension preheater.

This work relates to the exergy analysis and the study of the reduction of entropy production generated during the cooling of the clinker. Kunii-Levenspiel [6] proposed the representation of gas-solid continuous cross-flow heat exchange by a series of stages fully mixed cross-current contacting. Based on this configuration, the developed model allows the calculation of temperature profiles of the clinker, air and wall along the cooler which are inaccessible by experimental measurement considering the currently available techniques.

The equation of the entropy production in gas-gas counter-flow heat exchanger developed by Bejan [7] is applied to this gas-solid cross-flow heat exchanger. The model allows to calculate the entropy generation number for various values of the adimensional parameters under the real operating conditions as in the cement factory of Meftah.

2. COOLER DESCRIPTION AND ASSUMPTIONS

The clinker going out of the rotary kiln at a temperature of 1380°C is cooled by the air at a temperature of 65°C (Fig.1) by a cross-flow heat exchange with the top of the highly refractory steel grate. Thanks to an oscillatory movement, the grates cause the advancement and the spreading out of the clinker in a layer whose thickness depends on grate speed. After the crossing of the layer of clinker, the heated air is partly used as secondary air for the combustion of natural gas and partly evacuated towards the de-dusting system. The air depressions created at the entry and the exit of the exchanger divide the cooler, whose walls coating is made with refractory bricks, into two zones, named hot and cold zones. For the development of the model, the following assumptions are made, based on different studies [8-10]:

- the cooler is equipped with a rectangular roof provided with two exits,
- the clinker bed is uniform and rectangular in both hot and cold zone,
- the clinker consists of homogeneous spherical particles with an average diameter of 15 mm and of a bulk density of 1500 kg/m^3,
- the porosity of the clinker bed is supposed equal to 0.4,
- the initial temperature of the clinker on the first grate is equal to that one at the exit of the kiln,
- the distribution of the air in the bed is uniform,
- the air flow at the entry to the bed is characterized by a superficial velocity u_0 and an average pressure P_a,
- the quantities of fine particles transported by air flows and crossing the grates slits are negligible,

- the position of the limit between the hot and cold zones is fixed,
- the frequency of the grates movement in the cold zone ω_f is taken as the average frequency of grates in that zone.

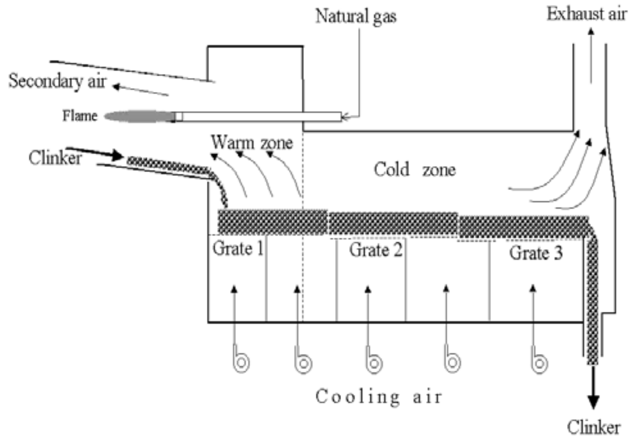

Figure 1. Scheme of the clinker cooler

3. EXERGY ANALYSIS OF THE COOLER

The identification of the exergy losses sources and their quantification allow the improvement and the optimization of an energy process [11]. It is considered that the flow of heat dissipation losses of the cooler are rejected to the ambient air with the temperature T_0. The exergy balance in steady state of the open system of clinker cooling (Fig. 2) is:

$$Ex_d = (m_{ck}\,\bar{e}_{ck,in} + m_{a1}\,\bar{e}_{a1} + m_{a2}\,\bar{e}_{a2}) - (m_{ck}\,\bar{e}_{ck,out} + m_{as}\,\bar{e}_{as} + m_{aexh}\,\bar{e}_{aexh}) + W \quad (1)$$

This equation includes three terms:

- The specific exergy ($\bar{e}$) associated to the clinker and the air
- The work rate flow (W) of the grates movement
- The flow exergy destroyed (Ex_d) due to the production of entropy generated by the irreversibilites of the system. It is defined by:

$$Ex_d = T_0\,S_{gen} \quad (2)$$

The coefficient of exergy efficiency of this system, based on the concept of transiting exergy [12], is given by Eq. (3):

$$\eta_e = \frac{m_{as}\,\bar{e}_{as} + m_{aexh}\,\bar{e}_{aexh} + m_{ck}\,\bar{e}_{ck,out} - E^{tr}}{m_{ck}\,\bar{e}_{ck,in} + m_{a1}\,\bar{e}_{a1} + m_{a2}\,\bar{e}_{a2} + W - E^{tr}} \quad (3)$$

Where, E^{tr} represents the thermo-mechanical transit exergy which passes through the cooler without undergoing any transformation or qualitative change. It is defined at the lowest values of pressure and temperature at inlet or outlet. It is computed by Eq. (4):

$$E^{tr}_{(P,T)} = m_{a1}\,\bar{e}_{a1}(P_{aexh}, T_{a1}) + m_{a2}\,\bar{e}_{a2}(P_{as}, T_{a2}) + m_{ck}\,\bar{e}_{ck,out} \quad (4)$$

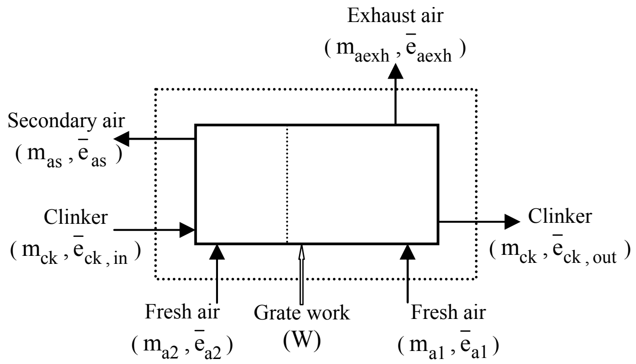

Figure 2. Mass and Exergy flow diagram of clinker cooler

From the function of the physical exergy [13], the specific exergies at (T,P) of the clinker and the humid air are respectively expressed by Eqs. (5) and (6):

$$\bar{e}_{ck} = (\bar{h}_{ck} - \bar{h}_0) - T_0\,(\bar{s}_{ck} - \bar{s}_0) \quad (5)$$

$$\bar{e}_a = (\bar{h}_a - \bar{h}_0) - T_0\,(\bar{s}_a - \bar{s}_0) \quad (6)$$

The dead state is characterized by (T_0 , P_0); T_0 is the ambient temperature equal in this case to 298K, P_0 is the atmospheric pressure. The kinetic and potential exergies are neglected.

Since the clinker and the humid air are considered as ideal mixtures of pure substances and perfect gases (see Table 1), the specific exergies are calculated by Eqs. (7) and (8):

$$\bar{e}_{ck} = \sum_{i=1}^{9} X_i \left(\int_{T_0}^{T} Cp_i(T)\,dT - T_0 \int_{T_0}^{T} Cp_i(T)\,d\ln(T) \right) \quad (7)$$

$$\bar{e}_a = \sum_{i=10}^{12} X_i \left(\int_{T_0}^{T} Cp_i(T)\,dT - T_0 \left[\int_{T_0}^{T} Cp_i(T)\,d\ln(T) - \frac{R}{M_i} \ln\frac{P}{P_0} \right] \right) \quad (8)$$

where, the mass fraction X_i of component i is given in Table 1.

The specific heat of component i [14] is expressed according to the temperature by Eq. (9):

$$Cp_i(T) = a_i + b_i\,T + c_i\,T^{-2} \quad (9)$$

With Eqs. (7), (8) and (9), the specific exergies of various streams are calculated according to real operating conditions of the Meftah cement factory. The transiting thermo-mechanical exergy of air and clinker traversing the cooler can be neglected, it constitutes 0.44 % of the overall exergy input. The coefficient of exergy efficiency of the cooler (Fig. 3) remains lower than 50% whereas the energy efficiency calculated for a similar system is about 85 % [15]. This highlights the importance of the exergetic approach in the optimization of the energy process. Cooling causes an internal exergy losses of 50.68 %. This considerable loss of exergy characterizes the irreversibility of heat exchange between the air and the clinker, from which the interest to determine the causes of these thermodynamic imperfections in heat transfer. The produced utilizable exergy [16] of secondary air represents 43.80 % of the total exergy input.

Table 1. Mass fraction of clinker and air constituents

	Clinker									Air		
	C_3S	C_2S	C_3A	C_4AF	CaO	MgO	K_2O	Na_2O	$CaSO_4$	O_2	H_2O	N_2
Mass fraction (%)	60.83	17.06	9.53	9.12	0.09	1.03	0.92	0.30	1.12	23	1	76
Indices (i)	1	2	3	4	5	6	7	8	9	10	11	12

The exhaust air conveys an external exergy losses of 5.08 % whose recovery can contribute to improve the exergetic performance of this system.

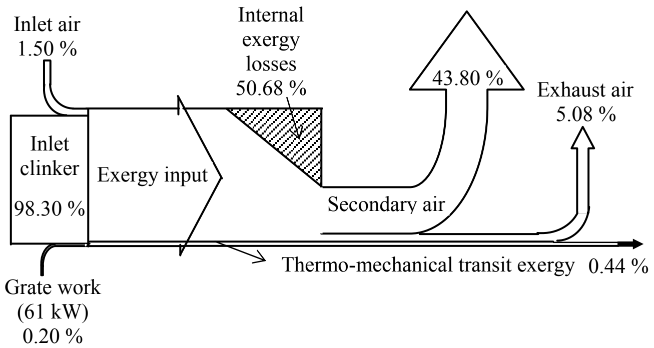

Figure 3. Cooler exergy balance

4. COOLER MODELING

The clinker cooling in steady-state conditions is modelled by a series of contactors (Fig. 4) with a perfect cross-flow heat exchange [6]. The heat transfer and the pressure drop are defined by correlations referring to macroscopic hydrodynamic criteria. The number of stages in the warm zone (K) and the cold one (N-K) are determined by the Eqs. (10) and (11) as a function of the residence time of the clinker in each stage $\bar{t}$ equal to the overall residence time divided by N.

$$K = \frac{H_c\ L_c\ \ell\,\rho_{ck}}{m_{ck}}\,\frac{1}{\bar{t}} \tag{10}$$

$$(N\text{-}K) = \frac{H_f\ L_f\ \ell\,\rho_{ck}}{m_{ck}}\,\frac{1}{\bar{t}} \tag{11}$$

The heights of the bed are expressed according to the frequency of the grates by Eqs. (12) and (13):

$$H_c = \frac{m_{ck}}{C\ \omega_c\ \rho_{ck}\ \ell} \tag{12}$$

$$H_f = \frac{m_{ck}}{C\ \omega_f\ \rho_{ck}\ \ell} \tag{13}$$

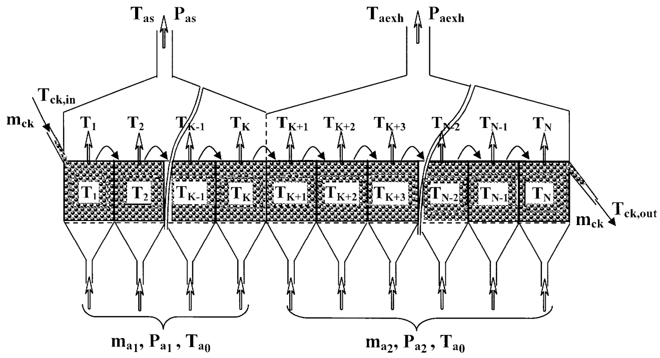

Figure 4. Clinker cooling in multiple crosscurrent contacting beds

It is considered that the clinker bed is fixed [8] that the pressure drop can be expressed by Ergun [17] Eq. (14) in which the loss of viscous energy is neglected.

$$\frac{\Delta P}{H} = 1.75\,\frac{(1-\beta)\,\rho_a\,u_0^2}{\beta^3\,\overline{dp}} \tag{14}$$

The density of air ρ_a is given by Eq. (15):

$$\rho_a = \frac{P_a}{rT} \tag{15}$$

with:

$$r = \frac{R}{\sum_{i=10}^{12} X_i\,M_i} \tag{16}$$

The energy balance for stage j (Fig. 5) is given by:

$$m_{ck}\,\bar{h}_{ck_{j-1}} + m_{a_j}\,\bar{h}_{a_0} = m_{ck}\,\bar{h}_{ck_j} + m_{a_j}\,\bar{h}_{a_j} + Q_{p_j} \tag{17}$$

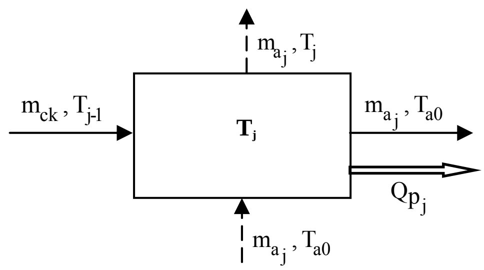

Figure 5. Energy balance of stage j

where, Q_{p_j} is the flow of the heat dissipation losses crossing the walls of the stage j which is expressed by:

$$Q_{p_j} = \frac{1}{R_{T_j}} \left(T_{p_j} - T_0 \right) \tag{18}$$

where, R_{T_j} is the total thermal resistance given by:

$$R_{T_j} = \frac{1}{A_j} \left(\frac{t_{br}}{\lambda_{br}} + \frac{t_s}{\lambda_s} + \frac{1}{h_c} \right) \tag{19}$$

In addition, by using the total heat transfer coefficient h_{f_j} between the medium and the wall for stage j, the flow of the heat dissipation losses can also be expressed by the following equation:

$$Q_{p_j} = h_{f_j} A_j \, (T_j - T_{p_j}) \tag{20}$$

The natural convection heat transfer coefficient h_c is given by the empirical correlation hereafter [18]:

$$Nu = 0.0295 \, Re^{4/5} \, Pr^{1/3} \tag{21}$$

In addition, assuming that the transfer of heat between the medium and the wall of the stage is carried out only by radiation between surfaces of clinker and the coating, h_{f_j} can be evaluated by:

$$h_{f_j} = \sigma \, \varepsilon_{ck} \varepsilon_{br} \frac{T_j^4 - T_{p_j}^4}{T_j - T_{p_j}} \tag{22}$$

in which emissivities of the coating and the clinker are respectively equal to 0.7 and 0.8 [19]. The mixture of air flows at the exit of each stage allows the calculation of the temperatures of the secondary and the exhaust air (T_{as}, T_{aexh}).

5. RESOLUTION AND RESULTS

5.1 Resolution

The model calculates the temperatures of the clinker, the air and the wall along the cooler, on the basis of conceptual parameters of the model (N, K) and of the operational data. The process with multistage cross currents requires the initialization of the average residence time $\bar{t}$ for the calculation of the number of stages. The resolution of the equations of the model proceeds in two steps; the calculation of the temperatures of the medium and the wall of the various stages. the temperatures of the stages are calculated by Newton-Raphson method.

5.2 Results and discussion

The validation of the model is carried out by comparing the data of measurements and model (Table 3). A deviation lower than 5% for the temperature and the pressure is observed. It can be concluded that such a model based on the configuration of Kuni-Levenspiel [6] is suitable to predict the continuous cooling of the clinker in this type of set.

Table 3. Theoretical and experimental data of cooler

Parameters	Units	Real cooler	Model
Clinker outlet temperature	° C	65	68
Secondary air temperature	° C	840	810
Exhaust air temperature	° C	154	147
Secondary air pressure	bar	1.016	0.966
Exhaust air pressure	bar	1.011	0.976

The temperature profiles along the cooler of the clinker and of the air at the top of the bed are represented in Fig.6, the wall temperature profile is reported on Fig.7. These temperatures decrease according to an exponential law from the entry towards the exit of the cooler. The cooling rate for the clinker varies from 85°C/min in the hot zone to 25°C/min in the cold zone. This confirms that the hot zone is a zone of heat recovery used for the pre-heating of the air for the combustion step. This representation is in agreement with the design of the cooling process. In spite of the importance of the heat recovery rate in this zone, the improvement of the quality of the thermal transfer would be possible bringing closer the air temperature profile with the clinker one. The wall temperature decreases more quickly in the hot zone compared to the cold one. This is due to the intensity of the thermal losses by radiation in this hot zone. Nevertheless, the refractory brick lining ensures a good heat insulation.

6. ENTROPY PRODUCTION ANALYSIS IN THE HOT ZONE

According to the second principle of thermodynamics, the irreversibility losses always occur in real energy transfer conditions. The entropy balance is necessary to evaluate the production of entropy generated by the irreversibilities of heat exchange between the air and the clinker. By neglecting the flow of heat dissipation losses of the cooler, the entropy balance for stage j in the hot zone is given by the Eq. (23):

$$S_{gen\,j} = m_{ck} \, (\bar{s}_{ck\,j} - \bar{s}_{ck\,j-1}) + m_{a_j} \, (\bar{s}_{a_j} - \bar{s}_{a0}) \tag{23}$$

In the calculation of specific entropy, assuming that the average specific heat of the clinker and of the air are constant [13], the Eq. (23) becomes:

$$S_{gen_j} = m_{a_j} \overline{Cp_a} \ln\frac{T_j}{T_{a0}} + m_{a_j} \, r \ln\frac{P_{a1}}{P_{as}} + m_{ck} \overline{Cp_{ck}} \ln\frac{T_j}{T_{j-1}} \tag{24}$$

The sum of entropy rate production in K stages is thus:

$$S_{gen.} = \sum_{j=1}^{K} m_{a_j} \overline{Cp_a} \, Ln\frac{T_j}{T_{ao}} + \sum_{j=1}^{K} m_{a_j} \, r \, Ln\frac{P_{a1}}{P_{as}} + \sum_{j=1}^{K} m_{ck} \overline{Cp_{ck}} \, Ln\frac{T_j}{T_{j-1}} \tag{25}$$

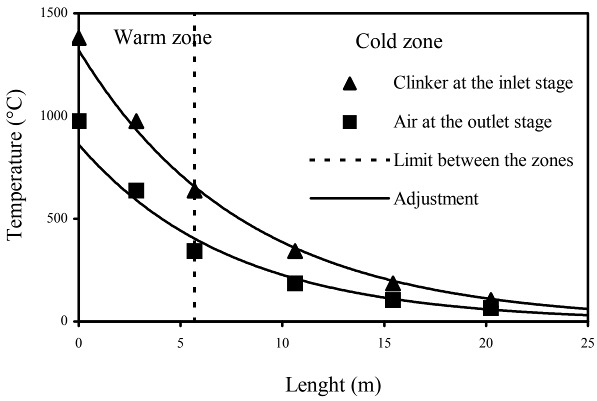

Figure 6. Computed clinker and air temperatures profiles

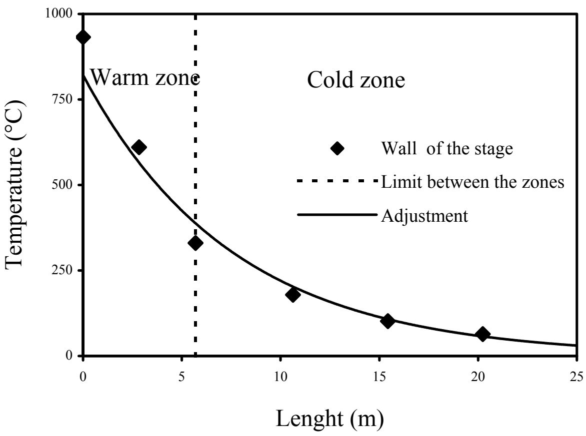

Figure 7. Computed wall temperature along the cooler

The entropy rate production due to the mixing effect of air flows at the exit of each stage at the top of the bed is given by:

$$S_{gen,\,mix} = \sum_{j=1}^{K} m_{a_j}\ \overline{Cp}_a\ \text{Ln}\,\frac{T_{as}}{T_j} \tag{26}$$

The entropy rate production in the hot zone is expressed by:

$$S_{gen.total} = \sum_{j=1}^{K} m_{a_j}\ \overline{Cp}_a\ \text{Ln}\frac{T_j}{T_{a0}} + \sum_{j=1}^{K} m_{a_j}\ r\ \text{Ln}\frac{P_{a1}}{P_{as}} + \sum_{j=1}^{K} m_{ck}\ \overline{Cp}_{ck}\ \text{Ln}\frac{T_j}{T_{j\text{-}1}} + \sum_{j=1}^{K} m_{a_j}\ \overline{Cp}_a\ \text{Ln}\frac{T_{as}}{T_j} \tag{27}$$

In the process considered, the pressure drop is negligible compared to the pressure at the entry of the bed, and the ratio of the pressures is written:

$$\text{Ln}\frac{P_{as}}{P_{a1}} = \text{Ln}\left(1-\frac{\Delta P}{P_{a1}}\right) = -\frac{\Delta P}{P_{a1}} \tag{28}$$

In addition, the efficiencies of heat utilization of clinker and air are expressed by Eqs. (29) and (30) [6]:

$$\eta_{ck} = \frac{T_K - T_{ck,\,in}}{T_{a0} - T_{ck,\,in}} = 1 - \frac{1}{(1+\phi)^K} \tag{29}$$

$$\eta_a = \frac{T_{a0} - T_{as}}{T_{a0} - T_{ck,\,in}} = \frac{1}{K\phi}\left[1 - \frac{1}{(1+\phi)^K}\right] \tag{30}$$

where the ratio of heat capacity rates is expressed by the Eq. (31):

$$\phi = \frac{m_a\ \overline{Cp}_a}{m_{ck}\ \overline{Cp}_{ck}} \tag{31}$$

To simplify the Eq. (27), the adimensional parameters are used:

$$\tau = \frac{T_{ck,\,in}}{T_{a0}} \tag{32}$$

$$H^* = \frac{H}{d_p} \tag{33}$$

$$N_S = \frac{S_{gen,\,total}}{m_a\ \overline{Cp}_a} \tag{34}$$

$$u_a^* = \frac{m_a}{L_c\ \ell\ \sqrt{2\,\rho_{a1}\,P_{a1}}} \tag{35}$$

where
τ: the absolute temperature ratio at the cooler entry,
H^*: the bed height on the average particle diameter,
u_a^* : the adimensional mass velocity of the air [7],
N_s : the entropy generation number defined by Bejan [20] for the evaluation of the degree of the irreversibilities of the set.

Introducing the Eqs. (14, 28- 35) into the Eq. (27), one obtains:

$$N_S = \text{Ln}\left[(1\text{-}\eta_a) + \eta_a\tau\right] + \text{Ln}\left[(1\text{-}\eta_{ck}) + + \eta_{ck}\left(\frac{1}{\tau}\right)\right] + \left[\frac{1}{K\phi} - 1\right]\ \text{Ln}\left[(1-\eta_{ck}) + \eta_{ck}\,\frac{1}{\tau}\right] + A\ u_a^{*2}\ H^* \tag{36}$$

where $A = \frac{3.5\,r}{\overline{Cp}_a}\,\frac{(1-\beta)}{\beta^3}$

is a presumedly constant adimensional factor.

This equation represents the entropy generation number N_S for the configuration of Kuni-Levenspiel in the case of this gas-solid heat transfer. This number (N_S) depends on τ, H^*, u_a^*, K and ϕ.

7. OPERATIONAL PARAMETERS EFFECT ON ENTROPY PRODUCTION

The sensitivity of the entropy generation number in the hot zone is studied under various operating conditions (Table 4) of clinker cooling.

Table 4. Variation of the operational parameters

Parameters	Units	Domain of variation
Particle diameter	m	0.005 ÷ 0.03
Grate frequency	s^{-1}	0.03 ÷ 0.15
Cooling air pressure	bar	1.032 ÷ 1.113
Cooling air flow rate	kg/s	21.49 ÷ 30.69
Cooling air temperature	° C	10 ÷ 60

The entropy generation number increases linearly as the ratio of the inlet absolute temperatures increases (Fig. 8). Sekulic [21] highlights the influence of the inlet temperature ratio on the quality of the energy transfer for various types of exchangers. Despite of all the calories recovery, this cooling does not restore to the air the initial hot clinker temperature (Fig. 6). Consequently this fall of temperature level causes an internal exergy losses. It is not convenient to cool clinker with air at low temperature, but at an optimal high temperature corresponding to a minimum entropy generation.

The tests of simulation carried out for stages 1 and 2 (Fig. 9) according to the ratio of the heat capacity rates show a weak reduction in the entropy generation number. The specific heat of the clinker to 1380°C is higher than that of the air with 25°C, arrangement in the air flow by the increase in its heat capacity rate attenuates the irreversibilities of this transfer.

The mass velocity of the air and the ratio height of the bed on the average diameter of clinker particle do not have practically any effect on the entropy generation number. (Figs. 10 and 11). As these two parameters characterize the pressure losses due to hydraulic friction, consequently the production of entropy generated by the pressure loss is negligible. For the whole tests carried out and for a value of the parameter considered, the increase in the number of stages representing the flow of the clinker is always favorable to the reduction in the production of entropy. Nevertheless its effect remains less significant than that of the absolute temperature ratio.

CONCLUSION

The exergy analysis allows the identification of the exergetic losses in the grate cooler of the cement facility of Meftah. These losses are estimated at 50.68 % on the level of heat exchange between the air and the clinker and of 5.08 % for the exhaust air. The model developed for heat exchange in this system, based on the representation of Kuni-Levenspiel, is validated by experimental data. The temperature profiles of the clinker, air and wall of the coating have been calculated. The setting in equation of the production entropy in this heat transfer, according to the representation of Kuni-Levenspiel, highlighted some adimensional parameters influencing the number of entropy production. The results of sensitivity tests, under the real operation conditions of the cooler, show that the entropy production of the cooler decreased by increasing the cooling air temperature. The heat recovery of the exhaust air will contribute to the pre-heating of the cooling air and decreasing the external exergy losses. On the basis of finite-time thermodynamics method, the optimal air temperature will be determined in further works.

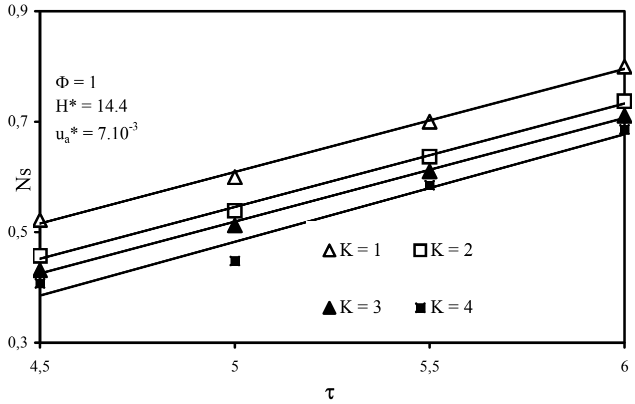

Figure 8. Effect of inlet temperature ratio

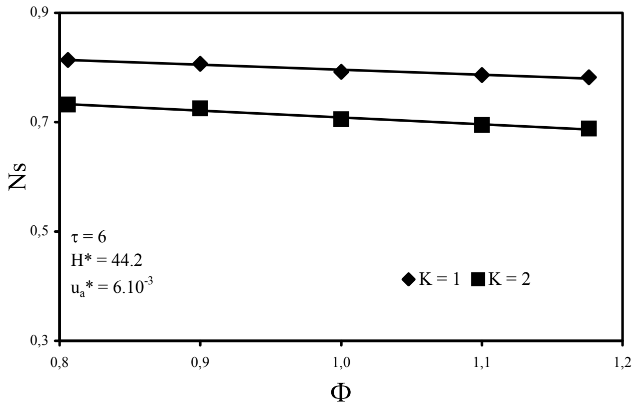

Figure 9. Effect of dimensionless mass velocity

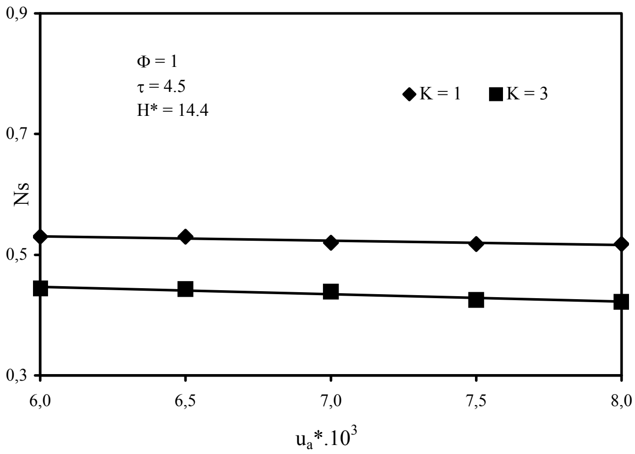

Figure 10. Effect of dimensionless mass velocity

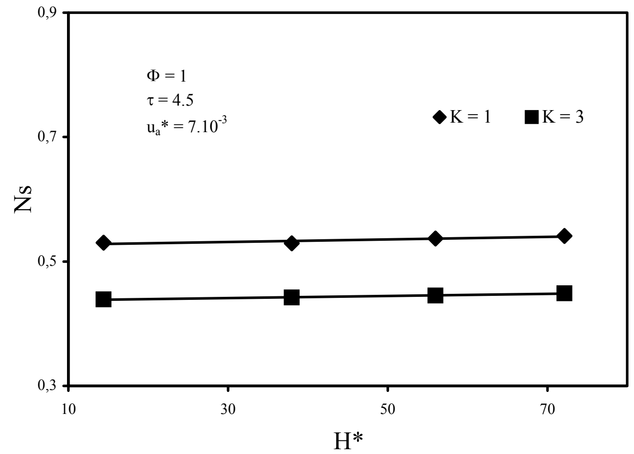

Figure 11. Effect of height and particle diameter ratio

ACKNOWLEDGEMENTS

The authors would like to acknowledge the support of the Mitidja Cement Compagny (SCMI) through the joint research project with the University of Blida.

REFERENCES

1. R. Frankenberg, The exergetic assessment of cement burning, *Zement-Kalk-Gips,* vol. 1, pp. 24-30, 1967.
2. B. Appelbaum and A. Lannus, Available energy analysis of dry process cement plant, *AICHE, 85 th Nat. Meeting*, A9, pp. 1-43, June, Philadelphia, U.S.A, 1978.
3. D. Touil, Les bilans d'énergie et d'exergie dans l'industrie de ciment, *Ciments, Bétons, Plâtres, Chaux*, vol. 4/815, pp. 250-253, 1995.
4. A. Gharsalli, Analyse exergeco-économique de l'atelier de cuisson de la cimenterie de SOTACIB, *Entropie*, vol. 219, pp. 47-52, 1999.
5. A. Bejan, Entropy generation minimization, the new thermodynamics of finite-size devices and finite-time processes , *J. Appl. Phys.*, 79, pp. 1191-1218, 1996.
6. D. Kunii and O. Levenspiel, *Fluidization Engineering*, John Wiley, New York, 1969.
7. A. Bejan, *Entropy generation through Heat and Fluid flow*, John Wiley, New York, 1982.
8. G.L. Bernstein, A Fundamental approach to grate coolers, *Zement-Kalk-Gips International,*vol. 3, pp. 125- 136, 1995.
9. H.P. Elkjaer, Boerkop and T. Enkegaard, Operation of grate coolers and a method of evaluating their efficiency, *Zement-Kalk-Gips International,* vol. 45, 10, pp. 510- 518, 1992.
10. K.V. Wedel, Neusdadt, R. Wagner and Clausthal, Are the grates clinker coolers or heat recuperators ? Limits of cross flow cooling in theory and practice, *Zement-Kalk-Gips International,*vol. 37, 5, pp. 244 - 247, 1984.
11. D.A. Rasheva and L.G. Atanasova, Exergy efficiency evaluation of the production of sulfuric acid from liquid sulfur, *Exergy, an International Journal*, vol 2. pp. 51-54, 2002
12. V.M. Brodyansky, M. Sorin and P. LeGoff, *The efficiency of industrial processes*, *Exergy Analysis and Optimisation,* Elsevier, Amsterdam, 1994.
13. T.J. Kotas, *The Exergy Method of Thermal Plant Analysis*, Butterworths, London, 1985.
14. I. Barin, O. Knacke and O. Kubachewsky, *Thermochemical Properties of Inorganic Substances*, Springer Verlag, Berlin, 1977.
15. L.T. Fan, Thermodynamically based analysis and synthesis of chemical process system, *Energy*, vol.5 pp. 955-966, 1980.
16. M. Sorin, J. Lambert and J. Paris, Exergy flow analysis in chemical reactors, *Trans. Inst. Chem. Engs.,* vol. 76, part A, pp 389-395, 1998.
17. S. Ergun, Fluid flow through packed columns, *Chem. Eng. Progress*, vol. 48, pp. 89-94, 1952.
18. C. Perry, *Chemical Engineering Handbook*, fourth edition, MacGraw Hill, NewYork, 1980.
19. A. Folliot, La transmission de chaleur dans le four rotatif à ciment, *Revue des Matériaux*, vol. 542, 1955.
20. A. Bejan, The concept of irreversibility in heat exchanger design: counter flow heat exchangers for gas-gas applications, *ASME J. Heat Transfer*, vol. 99, pp. 374-380, 1977.
21. D.P. Sekulic, The second law quality of energy transformation in a heat exchanger, *J. Heat Transfer*, 112, pp. 295-300, 1990.

NOMENCLATURE

Latin Symbols

A	average heat transfer area	m^2
C	distance covered by the grate	m
Cp	specific heat at constant pressure	$kJ\ kg^{-1}\ K^{-1}$
$\overline{Cp}$	average specific heat	$kJ\ kg^{-1}\ K^{-1}$
$\overline{d_p}$	mean diameter of particle	m
E^{tr}	thermo-mechanical transit exergy	kW
Ex_d	flow exergy destroyed	kW
$\bar{e}$	specific exergy	$kJ\ kg^{-1}$
H	bed height	m
H*	bed height on particle diameter	
h_c	average natural convectif heat transfer coefficient	$W\ m^{-2}\ K^{-1}$
h_f	average heat transfer coefficient	$W\ m^{-2}\ K^{-1}$
$\bar{h}$	specific enthalpy	$kJ\ kg^{-1}$
L	bed length	m
ℓ	bed width	m
M	molecular weight	$kg\ mol^{-1}$
m	mass flow rate	$kg\ s^{-1}$
u_a^*	dimensionless mass velocity	
Ns	entropy generation number	
Nu	Nusselt number	
P	pressure	Pa
Pr	Prandt number	
Q_p	flow of heat dissipation losses	kW
R	ideal gas constant	$J.kg^{-1}\ K^{-1}$
Re	Reynolds number	

R_T	thermal resistance	$[W\ m^{-2}\ K^{-1}]^{-1}$
S_{gen}	entropy generation rate	$kW\ K^{-1}$
$\bar{s}$	specific entropy	$kJ\ kg^{-1}\ K^{-1}$
T	temperature	K
Tp	wall temperature	K
t	thickness	m
$\bar{t}$	average residence time	s
u_0	superficial velocity	$m\ s^{-1}$
W	work rate flow of grate	kW
X	mass fraction	

Greek symbols

ΔP	pressure drop	Pa
β	bed porosity	
ε	surface emissivity	
ϕ	ratio of capacity rates	
η	efficiency of heat utilization	
η_e	exergy efficiency	
λ	thermal conductivity	$W\ m^{-1}\ K^{-1}$
ρ	density	$kg\ m^{-3}$
σ	constant of Stephan-Boltzmann	
τ	absolute temperature ratio	
ω	grate frequency	s^{-1}

Subscripts

i	i th component
j	j th stage
ck	clinker
a	air
aexh	exhaust air
as	secondary air
br	refractory brick
in	inlet
out	outlet
s	shell wall
c	warm zone
f	cold zone
0	dead state